Paleoceanography and Paleoclimatology

RESEARCH ARTICLE
10.1029/2020PA003998

Recent Constraints on MIS 3 Sea Level Support Role of Continental Shelf Exposure as a Control on Indo-Pacific Hydroclimate

T. Pico[1], D. McGee[2], J. Russell[3], and J. X. Mitrovica[4]

[1]Geological & Planetary Sciences, California Institute of Technology, Pasadena, CA, USA, [2]Earth, Atmospheric, and Planetary Sciences, Massachusetts Institute of Technology, Cambridge, MA, USA, [3]Earth, Environmental, & Planetary Sciences, Brown University, Providence, RI, USA, [4]Earth & Planetary Sciences, Harvard University, Cambridge, MA, USA

Key Points:
- Recent constraints suggest higher MIS 3 global mean sea level than in prior reconstructions
- We calculate continental shelf exposure in the Sunda and Sahul shelves from MIS 3 to the Last Glacial Maximum
- Our results negate prior criticisms of the hypothesis that continental shelf exposure controls rainfall variability over the Indo-Pacific

Supporting Information:
- Supporting Information S1
- Data Set S1
- Data Set S2
- Data Set S3
- Data Set S4

Correspondence to:
T. Pico,
tpico@caltech.edu

Citation:
Pico, T., McGee, D., Russell, J., & Mitrovica, J. X. (2020). Recent constraints on MIS 3 sea level support role of continental shelf exposure as a control on Indo-Pacific hydroclimate. *Paleoceanography and Paleoclimatology*, *32*, e2020PA003998. https://doi.org/10.1029/2020PA003998

Received 5 FEB 2020
Accepted 29 JUL 2020
Accepted article online 4 AUG 2020

Abstract The mechanisms controlling changes in atmospheric circulation and rainfall over the Indo-Pacific Warm Pool (IPWP) on glacial-interglacial timescales remain a subject of considerable debate. Continental shelf exposure, through sea-level drawdown during glacial periods, has been proposed as an important and possibly dominant control on rainfall intensity over the IPWP and Indian Ocean. However, longer records of hydroclimate change undermine this shelf exposure hypothesis. In particular, trends in some proxy records of rainfall do not track the extent of continental shelf exposure inferred from global benthic oxygen isotope records during Marine Isotope Stage 3 (MIS 3). We revisit the hypothesis that continental shelf exposure controls IPWP precipitation using the latest constraints on ice-age sea level. Recent studies on the timing and magnitude of global mean sea level during mid-MIS 3 (~45) suggest significantly higher peak sea level relative to previous work. Our gravitationally self-consistent glacial isostatic adjustment sea-level reconstructions, which adopt recent constraints on MIS 3 sea level, predict a transition from widely inundated to exposed shelves in the Indo-Pacific region from mid-MIS 3 to the beginning of the Last Glacial Maximum (LGM, ~19–26 ka). Over this same time period, proxy records of vegetation and hydrology from central Indonesia suggest a transition from wetter conditions during mid-MIS 3 to drier conditions during the LGM. Our new calculations thus negate prior criticisms related to the timing and extent of shelf exposure, indicating that shelf exposure may remain an important driver for hydroclimate variability in the IPWP region on glacial-interglacial timescales.

1. Introduction

The Indo-Pacific Ocean/Warm Pool is a critical component of the Earth's climate system as it contributes a substantial fraction of the global atmospheric moisture and energy budget (Hendon, 2003). In addition to being the largest source of atmospheric water vapor and experiencing the highest rainfall rates in the world, it has an important influence on global-scale climate through ocean-atmospheric interactions (Deser & Wallace, 1990). The region plays a key role in global erosion due to heavy rainfall, warm temperatures, high elevation relief, and widespread exposure of basalt, with some of the highest silicate weathering rates per unit area in the world (Milliman & Farnsworth, 2011). Silicate weathering imposes a negative feedback on climate by sequestering carbon dioxide, thus modulating global temperatures and, in turn, rainfall intensity (Molnar & Cronin, 2015; Walker et al., 1981). Understanding how the Indo-Pacific hydrological system changed in Earth's past is therefore crucial to interpreting a variety of paleoclimate records and can elucidate the role of glacial-interglacial climate variability on global hydroclimate (Chiang, 2014). Although there is evidence suggesting substantial changes in the strength of circulation over the Indo-Pacific Warm Pool (IPWP) on orbital timescales, the dominant control on this variability remains contentious (McGee, 2020).

Sea level has been proposed as a primary control on orbital-scale changes in rainfall intensity and the strength of the IPWP convection. During periods of lower sea level, more expansive continental shelves in the Indo-Pacific region (including the Sunda and Sahul shelves) may have led to drier conditions by lowering evaporation rates from oceans (Boos, 2012; DiNezio et al., 2011). Global climate model (GCM) simulations also suggest that shelf exposure during sea-level drawdown weakens the Indian Ocean Walker Circulation; DiNezio and Tierney (2013) show that 11 of 12 GCMs predict widespread drying over the Maritime Continent in response to continental shelf exposure during sea-level drawdown (DiNezio &

Tierney, 2013). In simulations using the Community Climate System Model, version 1.2, cooler conditions over the shelf result in increased subsidence, and easterly wind anomalies tilt and shoal the eastern Indian Ocean thermocline, transporting cold water to the surface and, thus, stabilizing the Walker Circulation anomalies via an Indian Ocean Bjerknes feedback (DiNezio et al., 2018). This modeling suggests that exposure of Sahul Shelf (on the Australian continent) may be more important than Sunda Shelf exposure in perturbing atmospheric circulation and therefore precipitation patterns (DiNezio & Tierney, 2013; DiNezio et al., 2016). Since the Sunda and Sahul shelves constitute ~15% of global continental shelf area, these regions may have played an important role in glacial-interglacial hydroclimate.

Some records of IPWP hydrology indicate that the timing of shelf flooding during the last deglaciation matches transitions from dry conditions during the Last Glacial Maximum (LGM; 26 ka) to wet conditions during the Holocene (Ayliffe et al., 2013; Griffiths et al., 2009; Krause et al., 2019; Wicaksono et al., 2017). However, other records indicate alternative timings for deglacial IPWP hydrologic change (Carolin et al., 2013, and references therein; Russell et al., 2014) and invoke other factors (atmospheric CO_2, sea surface temperatures, ice sheet topography, insolation seasonality, in addition to shelf exposure) that changed during the deglaciation to explain regional rainfall changes.

In addition, a more serious challenge to the continental shelf exposure hypothesis is that longer records of hydroclimate change, extending back to 60 ka, show moisture balance changes that do not track sea-level variations inferred from global benthic oxygen isotope records (Carolin et al., 2013; Russell et al., 2014). Rainfall proxies show a transition from wet conditions during mid-Marine Isotope Stage 3 (MIS 3) to dry conditions at the LGM; however, most sea-level reconstructions predict extensive shelf exposure (low sea level) to continue from MIS 4 to the LGM. Studies such as Russell et al. (2014) interpreting these rainfall records have instead suggested that a threshold in ice sheet topography (Jones et al., 2018; Lee et al., 2015) or CO_2 atmospheric concentration (Ehlerginger et al., 1997) might control regional hydroclimate. However, recent constraints on the timing and magnitude of global mean sea level (GMSL; or, alternatively, ice volumes) during mid-MIS 3 (50–35 ka) suggest significantly higher peak sea level compared with previous reconstructions (Pico et al., 2017, 2016).

We seek to revisit the hypothesis that continental shelf exposure drives hydroclimate variability in light of improved estimates of MIS 3 global sea-level change. In particular, we perform glacial isostatic adjustment (GIA) simulations to predict regional sea-level change on the Sunda and Sahul shelves and calculate continental shelf exposure area over the last glacial cycle. We assess the consistency between our new calculations of shelf exposure area and records of past rainfall to determine whether sea-level change remains a viable mechanism to drive ice-age precipitation change over the IPWP. These recent sea-level constraints contribute to the ongoing debate on possible physical mechanisms controlling rainfall variability in the Indo-Pacific and highlight that continental shelf exposure should not yet be dismissed as a potential driver for rainfall changes in proxy records on glacial-interglacial timescales.

2. Background

2.1. Recent Advances in Ice-Age Sea Level

Understanding how sea level varied over the last ice age is crucial to accurately reconstructing Sahul and Sunda continental shelf exposure. Yet reconstructing a history of global ice volume across the last glacial buildup phase is a challenge due to the sparsity of geologic data constraining GMSL and continental ice extent (Clark et al., 1993; Siddall et al., 2008; Waelbroeck et al., 2002). During the glacial buildup phase, GMSL was lower than it is today, and subsequent sea-level rise during the last deglaciation (26 ka to present) destroyed or submerged the majority of sea-level records. A recent analysis of widely distributed sea-level records has constrained peak GMSL to be -11.6 ± 6.6 m during MIS 5c (~100 ka) and -10.5 ± 5.5 m during MIS 5a (~80 ka) (Creveling et al., 2017). However, it remains challenging to estimate GMSL during lowstands across the glacial cycle (MIS 5d, 5b, and 4; Cutler et al., 2003).

GMSL reconstructions based on scaling benthic oxygen isotope records, such as Waelbroeck et al. (2002), suggest a sea-level fall from MIS 3 to LGM, from −55 to −130 m. The average depth of the Sunda and Sahul shelves is ~40 m, and most analyses of continental shelf exposure have used these scaled oxygen isotope records to infer substantial continental shelf exposure during MIS 3. However, observations of sea level

dated to mid-MIS 3 (50–35 ka) indicate that GMSL experienced a peak highstand significantly closer to the modern level than implied by a simple scaling of oxygen isotope records (Cabioch & Ayliffe, 2001; Cann, 2000; Liu et al., 2009). Furthermore, recent studies of GIA have constrained the magnitude of the global sea-level fall leading into the LGM. In particular, an analysis of sediment core records from the Bohai Sea concluded that peak GMSL during MIS 3 reached -37.5 ± 7 m during mid-MIS 3 (50–37 ka), implying that ice volumes tripled from this period to the LGM (from −37.5 to −130 m GMSL) (Pico et al., 2016). Furthermore, an analysis of sea-level data on the U.S. east coast (Pico et al., 2017) supports field evidence for a substantial growth in the volume of the Laurentide Ice Sheet during MIS 3 (Carlson et al., 2018; Dalton et al., 2016, 2019). On the Sunda and Sahul shelves, where modest sea-level changes cause substantial shoreline migration, these differences in peak reconstructed GMSL during MIS 3 can substantially impact retrodictions of exposed shelf area; the recently revised, higher estimates for peak GMSL would suggest more extensive inundation of continental shelves in the Indo-Pacific at mid-MIS 3.

2.2. Proxy Records for Past Hydroclimate

Most proxy records indicate increasing rainfall in the Indo-Pacific during the last deglaciation (Reeves et al., 2013), but there are far fewer records that extend to MIS 3 to document trends in precipitation change prior to the LGM. However, recent sediment organic geochemical and speleothem oxygen isotope records do cover this interval. Speleothem oxygen isotope records track drip water composition from rainfall. Records from northern Borneo and Sulawesi show variability over the last ice age that do not appear to track sea-level changes (Carolin et al., 2013, 2016; Krause et al., 2019), and these $\delta^{18}O$ records will be further explored in the discussion.

Lake and marine sediment records from Sulawesi and offshore Sumatra are based on the $\delta^{13}C$ of leaf waxes, which is used to differentiate between plants that use C3 or C4 photosynthetic pathways. In the tropics, most grasses use the C4 photosynthetic pathway, a CO_2 concentrating mechanism that increases the efficiency of photorespiration and water use. Their $\delta^{13}C_{wax}$ is less negative than C3 plants, which include most trees. Thus, $\delta^{13}C_{wax}$ is interpreted as a proxy for the relative proportion of trees (C3) versus grasses (C4), recording forest/grassland transitions wherein more depleted values reflect wetter conditions (greater soil moisture) and positive values reflect drier conditions (Castaneda et al., 2009; Vogts et al., 2009). Although the abundance of C3 relative to C4 grasses can also be impacted by CO_2 availability and temperature (Diefendorf et al., 2010; Ehlerginger et al., 1997; Marshall et al., 2008), transitions between grasslands and forest are the dominant process recorded by $\delta^{13}C_{wax}$ records in the tropics and are much more strongly controlled by precipitation and, in particular, the intensity of the dry season (Dubois et al., 2014).

Figures 2b–2d show records of $\delta^{13}C_{wax}$ in three different locations in the Indo-Pacific region, including records in lake sediments in Sulawesi and marine sediments off the Sumatra coast (Russell et al., 2014; Wicaksono et al., 2015; Windler et al., 2019), which all show an increase in $\delta^{13}C_{wax}$ values beginning at mid-MIS 3 (50–35 ka).

3. Methods

3.1. GIA Simulations

To calculate regional sea-level changes and model the extent of continental shelf exposure through time, we model the spatiotemporal pattern of sea-level change as the solid Earth responds to the redistribution of ocean and ice mass loads in the process of GIA (Mitrovica & Milne, 2002). Our sea-level calculations are based on the theory and pseudo-spectral algorithm described by Kendall et al. (2005) with a spherical harmonic truncation at degree and order 512. These calculations include the impact of load-induced Earth rotation changes on sea level (Milne & Mitrovica, 1996; Mitrovica et al., 2005), evolving shorelines, and the migration of grounded, marine-based ice (Johnston, 1993; Kendall et al., 2005; Lambeck et al., 2003; Milne et al., 1999). Our numerical predictions require models for Earth's viscoelastic structure and the history of global ice cover. We adopt the VM2 Earth model (Peltier & Fairbanks, 2006) and test two different ice histories over the last glacial cycle.

We first use the ICE-PC2 global ice history (Pico et al., 2017), which includes recent estimates for the timing and magnitude of peak MIS 3 GMSL. This history is based on revising the standard ICE-5G ice history (Peltier & Fairbanks, 2006) in accordance with recent global ice volume constraints during the last

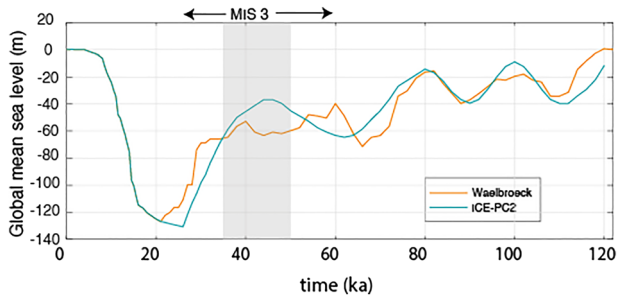

Figure 1. Global mean sea level associated with the Waelbroeck et al. (2002; orange) and ICE-PC2 (Pico et al., 2017; blue) ice histories over the last glacial cycle.

glaciation phase (blue; Figure 1). As in Pico et al. (2017), this global ice history is characterized by a peak GMSL value during MIS 3 of −37.5 m at 44 ka, following Pico et al. (2016), and −15 and −10 m during MIS 5a and 5c, respectively, which are within the ranges derived by Creveling et al. (2017). We construct a second ice history, which revises the standard ICE-5G ice history to fit the GMSL history proposed in Waelbroeck et al. (2002) on the basis of oxygen isotope records scaled to match the Huon peninsula sea-level record (Lambeck & Chappell, 2001) (orange; Figure 1); the latter GMSL history has been used in previous studies to compare hydroclimate records with estimated continental shelf exposure area in the Indo-Pacific region.

Our global simulations of GIA predict a spatially variable pattern of sea-level change over the last glacial cycle based on the input of two global ice volume histories, ICE-PC2 and Waelbroeck. Thus, our reconstruction for Sunda and Sahul shelf area accounts for local deviations from the globally averaged sea level at any given time (Figure 3).

3.2. Calculating Continental Shelf Area Over the Ice Age

We derive a time series of exposed continental shelf area over the last glacial cycle from our sea-level calculations. In Figure 2a, we track changes in continental shelf exposure area relative to today in the Sunda and Sahul shelves for calculations based on both the GMSL history proposed in Waelbroeck et al. (2002) (orange) and ICE-PC2 (blue). To determine shelf exposure, we reconstructed paleotopography at each simulated time step by subtracting the predicted relative sea-level change from that time step to the present day due to GIA from present-day topography (based on the NOAA ETOPO1 data set). We then calculated the area above sea level within a region bounded by −15°N, −15°S, 90°E, and 150°E. These continental shelf area calculations therefore account for shoreline migration due to spatially variable sea level driven by GIA.

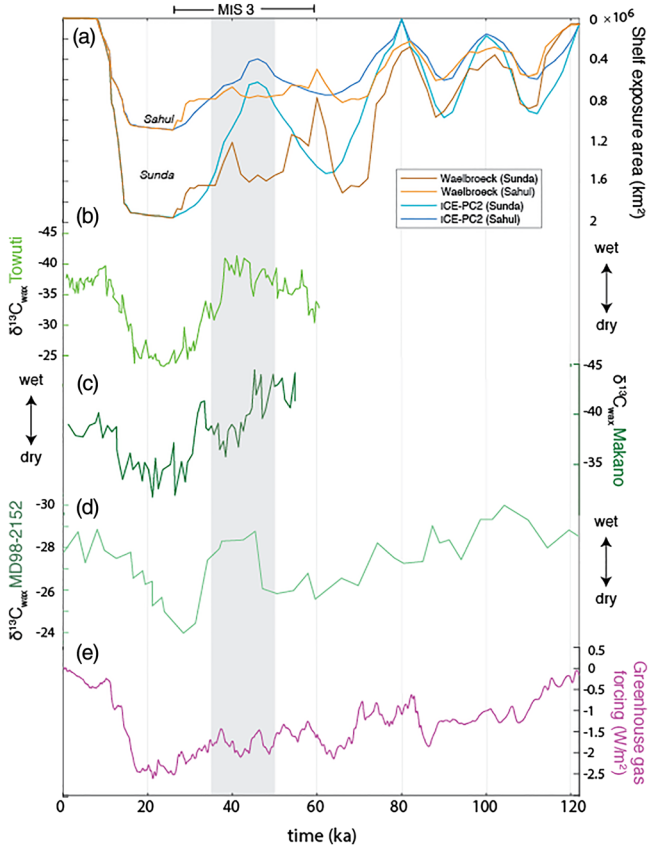

Figure 2. (a) Continental shelf exposure area is calculated from glacial isostatic adjustment simulations based on the ice histories in Figure 1 for the Sahul and Sunda shelves for Waelbroeck (orange) and ICE-PC2 (blue). Records of $\delta^{13}C$ in leaf waxes from (b) Lake Towuti (Russell et al., 2014), (c) Lake Matano (Wicaksono et al., 2015), and (d) MD98-2152 (purple; Windler et al., 2019). (e) Greenhouse gas forcing (W/m^2) from Schilt et al. (2010).

4. Results

4.1. Predicted Continental Shelf Exposure Area

We predict paleotopography and exposed shelf area during MIS 3 at 44 ka using GIA simulations with the Waelbroeck and ICE-PC2 ice histories (Figure 3; top) and compare to the paleotopography at the LGM (Figure 3; bottom). The shelf break in this region is close to −50 m, and so extensive submergence of shelves occurs when local sea level is higher than this threshold. During MIS 3, the regional relative sea-level prediction (i.e., sea level during MIS 3 relative to present-day sea level) based upon ICE-PC2 peaks at values that surpass this threshold and substantial areas of the Maritime Continent are submerged (top left, Figure 3); in particular, total land exposure at 44 ka relative to present-day falls to a minimum of 0.65×10^6 km^2 on the Sunda Shelf and 0.40×10^6 km^2 on the Sahul Shelf (blue; Figure 2a). Land exposure at the LGM relative to present day in these areas is predicted to be 2.0×10^6 km^2 and 1.1×10^6 km^2, respectively (Figure 2a; bottom left, Figure 3). Ice volumes across the same time window during mid-MIS 3 remain significantly greater in predictions based on the Waelbroeck ice history relative to ICE-PC2, and land exposure at 44 ka is consequently more extensive (top right, Figure 3): 1.55×10^6 km^2 in the Sunda Shelf and 0.8×10^6 km^2 in the Sahul Shelf (orange; Figure 2a).

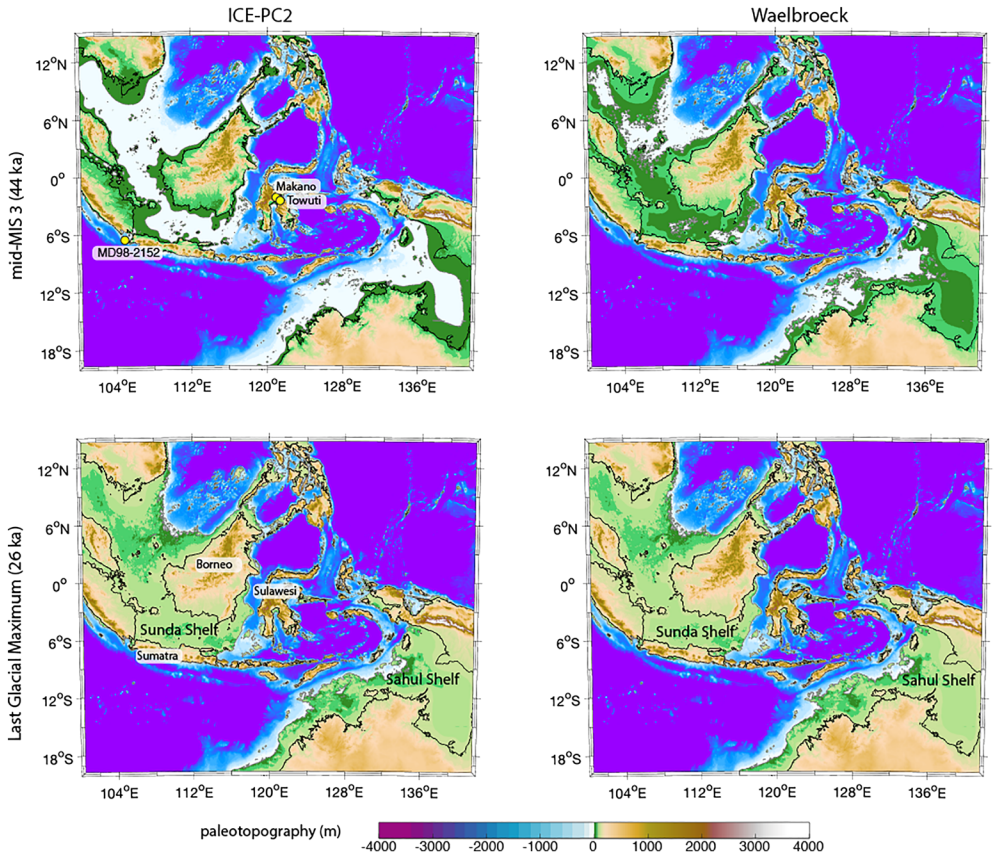

Figure 3. Paleotopography calculated from glacial isostatic adjustment simulations using ice history ICE-PC2 (left) and Waelbroeck (right) during mid-MIS 3 (44 ka; top) and at the Last Glacial Maximum (26 ka; bottom). Present-day shoreline is shown by black line, and paleoshoreline is shown by gray line. Locations where paleoclimate proxies were measured are shown by yellow circles in top left panel. Locations of Sumatra, Sulawesi, and Borneo are labeled on bottom left panel.

5. Discussion

The results in Figure 2a indicate that ICE-PC2, the recently revised model for GMSL during mid-MIS 3 (Pico et al., 2017, 2016), leads to a significantly greater (factor of ~3) increase in shelf exposure from mid-MIS 3 to LGM than the predictions based on earlier inferences of GMSL. Although the Waelbroeck ice history is characterized by a higher GMSL peak at 60 ka (comparable to the GMSL peak in ICE-PC2), this peak timing results in a slower rate of sea-level fall, and therefore continental shelf exposure, in the period leading to the LGM. When we compare the exposed continental shelf area retrodicted by the simulations based on the Waelbroeck and ICE-PC2 ice histories to the hydroclimate proxy records from $\delta^{13}C_{wax}$ (Figure 2a), we find a drying trend coincident with the sea-level drawdown associated with ice history ICE-PC2 from 50 to 35 ka to the LGM.

It is challenging to compare variations in continental shelf area across the entire glaciation phase to hydroclimate records since only one $\delta^{13}C_{wax}$ record (that from MD98-2152; Windler et al., 2019) extends through the last glacial cycle (Figure 2d). Nevertheless, this $\delta^{13}C_{wax}$ record shows depleted values, representing a wet period, at 100 ka, which coincides with greater submergence of the continental shelves (Figure 2d). This correlation suggests that continental shelf exposure might control previous intervals of wet to dry transitions, although the drying trend at 100 ka is of a smaller magnitude compared with that at mid-MIS 3. Improved constraints on GMSL during the glaciation phase, especially on GMSL lowstands such as MIS 5d, MIS 5b, and MIS 4, will aid in comparing predictions of sea-level change (and continental shelf exposure) to hydroclimate proxies further back in time. Nonetheless, existing $\delta^{13}C_{wax}$ records track changes in continental shelf exposure for the most recent constraints on the GMSL drawdown from mid-MIS 3 to the LGM.

5.1. Variability in Hydroclimate Records

The records in Figures 2b–2d all show an enrichment (more positive values) in $\delta^{13}C_{wax}$ beginning between 50 and 35 ka, indicating a drying climate, consistent with the timing of extensive shelf emergence. This timing does not coincide with variations in greenhouse gas forcing (Figure 2e), including atmospheric CO_2 concentrations as measured in Antarctic ice cores (Luthi et al., 2008). The magnitude of this excursion varies significantly between the records; however, this does not reject the continental shelf exposure hypothesis, as differences in $\delta^{13}C_{wax}$ magnitude are to be expected given the setting of the three records. Previous work on Sulawesi has shown that $\delta^{13}C_{wax}$ variations in marine records, such as that of Windler et al. (2019), are generally smaller than in terrestrial records, likely due to much larger source areas for waxes (Konecky et al., 2016; Wicaksono et al., 2015). Further, Wicaksono et al. (2015) show that the smaller amplitude of $\delta^{13}C_{wax}$ variations observed in Lake Matano relative to Lake Towuti is likely due to the higher elevation of Matano, which supports higher mean annual precipitation, as well as the geomorphology of Lake Towuti, which is more conducive to grasslands. Indeed, $\delta^{13}C_{wax}$ is not a quantitative indicator of precipitation, and models predict that precipitation variations driven by shelf exposure are not uniform over the IPWP (DiNezio et al., 2018).

Although enrichment (more positive values) at ~40 ka in these $\delta^{13}C_{wax}$ records is consistent with the hypothesis that continental shelf exposure drives rainfall variability, speleothem $\delta^{18}O$ records from the region show little change at this time. The $\delta^{18}O$ record from Gunung Buda, northern Borneo, indicates very gradual ^{18}O enrichment (more positive values) from ~60 until ~16 ka, without any clear shift between 50 and 35 ka (Carolin et al., 2013). A $\delta^{18}O$ record from Maros, Sulawesi, although shorter, indicates little change between 40 and ~16 ka (Krause et al., 2019). It is possible that the Sulawesi record captures only the latest stages of shelf exposure and therefore misses the main interval of drying, whereas the northern Borneo record may be most sensitive to changes in precipitation north of the Maritime Continent and Sunda Shelf, where precipitation changes could be weaker than further south, though modeling studies predict the opposite relationship (DiNezio et al., 2018).

Orbital forcing is another mechanism invoked to explain hydroclimate variability in the tropics (Clement et al., 2004). Changes in precession can influence rainfall patterns by changing seasonal cloudiness, either amplifying or reducing the meridional gradient in sea surface temperatures, and thereby Walker Circulation (Timmermann et al., 2007). Rainfall reconstructions from speleothem $\delta^{18}O$ records in northern Borneo are dominated by a precessional signal (Carolin et al., 2016; Meckler et al., 2012; Partin et al., 2007). Furthermore, these records document changes in rainfall coinciding with Heinrich events (Carolin et al., 2013). Rather than perturbations to Walker Circulation, these studies point to the role of precession in controlling the position of the Intertropical Convergence Zone (ITCZ), as suggested by modeling studies (Donohoe et al., 2013). Variations in precessional forcing, along with greenhouse gas forcing and ice albedo (DiNezio et al., 2016), thus also play a part in producing the rainfall variability inferred from $\delta^{13}C_{wax}$ records, in addition to continental shelf exposure, and isolating each of these mechanisms across the last glacial cycle should be a focus of future climate modeling.

Alternatively, recent work has suggested that precipitation isotope records from this region cannot be interpreted as simple records of rainfall amount due to a variety of "source effects," including changes in atmospheric vapor transport and isotope distillation related to exposure of the Sunda Shelf (Konecky et al., 2016; Wicaksono et al., 2015). Titanium count is another proxy for rainfall reconstructions, as it tracks continental erosion and runoff, and such reconstructions suggest a shift from wet to dry from mid-MIS 3 to the LGM, similar to the $\delta^{13}C_{wax}$ records (Costa et al., 2015; Russell et al., 2014). Future work that can quantitatively constrain precipitation amount changes would be instrumental in testing the effects of shelf exposure predicted by climate models. Nevertheless, the rainfall-sensitive vegetation records from the region suggest substantial drying associated with shelf exposure, consistent with model results (DiNezio & Tierney, 2013; DiNezio et al., 2016).

5.2. East African Precipitation Changes

In some GCM simulations, continental shelf exposure in the Indo-Pacific region leads to increased precipitation in Eastern Africa along with decreased precipitation over the Maritime Continent (DiNezio & Tierney, 2013). These simulations suggest that the impacts of continental shelf exposure extend beyond

the IPWP region and influence hydroclimate in more remote locations. If continental shelf exposure produces opposite-sign precipitation changes in East Africa compared with the Indo-Pacific, then we might expect drier conditions in East Africa during MIS 3 when the Maritime Continent is substantially flooded. There are few records that extend to MIS 3 from this region; however, existing records do not show transitions antiphased with the vegetation records from the Indo-Pacific region (Brown et al., 2007; Garcin et al., 2006; Tierney et al., 2017). Whereas 11 of 12 GCMs examined in DiNezio and Tierney (2013) predict widespread drying over the Maritime Continent in response to shelf exposure at the LGM, only half of these simulations show an East African hydroclimate response to sea-level changes, indicating a less robust response than over the IPWP. The climate changes predicted by these models are also dependent on greenhouse gas concentrations and climate boundary conditions governed by orbital configurations, which would have been different during the MIS 3 to LGM transition compared to the period from LGM to the Holocene. Thus, it remains unclear whether Indo-Pacific shelf exposure during MIS 3 should influence East African hydroclimate.

5.3. Implications for Geochemical Cycling Over the Ice Age

The Maritime Continent is characterized by substantial relief of mafic rocks and high rainfall intensity and is a significant contributor to the present-day silicate weathering budget of the Earth (Macdonald et al., 2019; Molnar & Cronin, 2015). In the silicate weathering feedback hypothesis, a drop in global CO_2 causes colder climates and less weathering (Walker et al., 1981). However, if continental exposure, rather than temperature, plays a key role in regional precipitation, then relative sea-level changes may have imposed a control on rainfall, and therefore silicate weathering, during the geologic past. Thus, the history of sea level in the region may be an important lever on the evolution of global silicate weathering through the ice age (McGee, 2020).

6. Conclusions and Future Work

In this study we reconsider the hypothesis that continental shelf exposure controls hydroclimate variability in the Indo-Pacific in light of recent constraints on GMSL during MIS 3. Our sea-level simulations, which account for GIA, predict an increase in exposed continental shelf area in the Indo-Pacific region from mid-MIS 3 to the LGM. Over this same time period, $\delta^{13}C_{wax}$ proxy records in Indonesia show a drying trend. The revised estimate of global mean sea-level fall from mid-MIS 3 to the LGM negates prior criticisms of the hypothesis that continental shelf exposure exerts a strong control on the vigor of atmospheric ascent and rainfall intensity over the IPWP. Our calculations suggest that sea-level changes remain, at least partially, a viable driver for rainfall proxy trends during MIS 3. Since a large proportion of total global precipitation falls in the Indo-Pacific region, a strong influence of shelf exposure on IPWP implies that a substantial amount of rainfall variability on glacial-interglacial timescales may be controlled by sea-level change rather than primarily by mean global temperature, ice sheet size, or other variables.

Future work should aim to better understand the relationship between rainfall intensity and shelf exposure in this region. Additional hydroclimate proxy records, in different locations and extending to MIS 5, will improve the interpretation of the role of sea level in IPWP convective intensity over the last glacial cycle. Improved understanding of sea-level change over the ice sheet growth phase of the last ice age will produce more accurate reconstructions of continental shelf exposure to compare against hydroclimate proxies. In particular, future work aimed at constraining global sea-level variability from MIS 5 through MIS 3, including the magnitude of global sea-level lowstands, may elucidate connections between ice sheets and global climate. Well-resolved sedimentary records, sampling depths between modern and LGM sea levels, have the potential to track past shorelines and therefore improve global mean sea-level reconstructions across the ice sheet buildup phase.

In addition, further work is needed to understand differences between various records of Maritime Continent hydroclimate over the last glacial cycle; as noted above, some records do not show drying from MIS 3 to the LGM (e.g., Carolin et al., 2013), and several records show transitions to wet conditions during the deglaciation that occur before substantial shelf flooding had occurred (e.g., Russell et al., 2014). It remains unclear whether these records reflect spatial variations or proxy-specific responses, or whether they are inconsistent with a dominant role for shelf exposure in controlling IPWP convection. Finally, the hypothesis that shelf exposure modulates Walker Circulation predicts precipitation changes of opposite

sign over easternmost tropical Africa. Future work constructing hydroclimate proxy records in this region through the last ice age might clarify the influence of shelf exposure on driving remote responses, such as in East Africa.

Data Availability Statement

Data sets for this research ($\delta^{13}C_{wax}$ records and continental shelf exposure area reconstructions) are included in this paper (and its supporting information) and are publicly available on Zenodo (citable using the DOI 10.5281/zenodo.3959364).

Acknowledgments

T. P. acknowledges funding from NSF-GRFP, NSF-EAR Postdoctoral Fellowship, and Harvard University. Research by J. R. on tropical climate variability is partially supported by the U.S. National Science Foundation. Conversations with J. Adkins improved the content of this manuscript. We appreciate thoughtful reviews by S. Carolin and an anonymous reviewer.

References

Ayliffe, L. K., Gagan, M. K., Zhao, J. X., Drysdale, R. N., Hellstrom, J. C., Hantoro, W. S., et al. (2013). Australasian monsoon during the last deglaciation. *Nature Communications*, *4*, 2908. https://doi.org/10.1038/ncomms3908

Boos, W. R. (2012). Thermodynamic scaling of the hydrological cycle of the Last Glacial Maximum. *Journal of Climate*, *25*(3), 992–1006. https://doi.org/10.1175/JCLI-D-11-00010.1

Brown, E. T., Johnson, T. C., Scholz, C. A., Cohen, A. S., & King, J. W. (2007). Abrupt change in tropical African climate linked to the bipolar seesaw over the past 55,000 years. *Geophysical Research Letters*, *34*, L20702. https://doi.org/10.1029/2007GL031240

Cabioch, G., & Ayliffe, L. K. (2001). Raised coral terraces at Malakula, Vanuatu, Southwest Pacific, indicate high sea level during marine isotope stage 3. *Quaternary Research*, *56*(3), 357–365. https://doi.org/10.1006/qres.2001.2265

Cann, J. H. (2000). Late Quaternary paleosealevels and paleoenvironments inferred from foraminifera, northern Spencer Gulf, South Australia. *The Journal of Foraminiferal Research*, *30*(1), 29–53. https://doi.org/10.2113/0300029

Carlson, A. E., Tarasov, L., & Pico, T. (2018). Rapid Laurentide ice-sheet advance towards southern last glacial maximum limit during marine isotope stage 3. *Quaternary Science Reviews*, *196*, 118–123. https://doi.org/10.1016/j.quascirev.2018.07.039

Carolin, S. A., Cobb, K. M., Adkins, J. F., Clark, B., Conroy, J. L., Lejau, S., et al. (2013). Varied response of western Pacific hydrology to climate forcings over the last glacial period. *Science*, *340*(6140), 1564–1566. https://doi.org/10.1126/science.1233797

Carolin, S. A., Cobb, K. M., Lynch-Stieglitz, J., Moerman, J. W., Partin, J. W., Lejau, S., et al. (2016). Northern Borneo stalagmite records reveal West Pacific hydroclimate across MIS 5 and 6. *Earth and Planetary Science Letters*, *439*, 182–193. https://doi.org/10.1016/j.epsl.2016.01.028

Castaneda, I. S., Mulitza, S., Schefuss, E., Lopes dos Santos, R. A., Sinninghe Damste, J. S., & Schouten, S. (2009). Wet phases in the Sahara/Sahel region and human migration patterns in North Africa. *Proceedings of the National Academy of Sciences*, *106*(48), 20159–20163. https://doi.org/10.1073/pnas.0905771106

Chiang, J. C. H. (2014). The tropics in paleoclimate. *Annual Review of Earth and Planetary Sciences*, *37*(1), 263–297. https://doi.org/10.1146/annurev.earth.031208.100217

Clark, P. U., Clague, J. J., Curry, B. B., Dreimanis, A., Hicock, S. R., Miller, G. H., et al. (1993). Initiation and development of the Laurentide and Cordillean ice sheets following the last interglaciation. *Quaternary Science Reviews*, *12*(2), 79–114. https://doi.org/10.1016/0277-3791(93)90011-A

Clement, A. C., Hall, A., & Broccoli, A. J. (2004). The importance of precessional signals in the tropical climate. *Climate Dynamics*, *22*, 327–341. https://doi.org/10.1007/s00382-003-0375-8

Costa, K. M., Russell, J. M., Vogel, H., & Bijaksana, S. (2015). Hydrological connectivity and mixing of Lake Towuti, Indonesia in response to paleoclimatic changes over the last 60,000 years. *Palaeogeography, Palaeoclimatology, Palaeoecology*, *417*, 467–475. https://doi.org/10.1016/j.palaeo.2014.10.009

Creveling, J. R., Mitrovica, J. X., Clark, P. U., Waelbroeck, C., & Pico, T. (2017). Predicted bounds on peak global mean sea level during marine isotope stages 5a and 5c. *Quaternary Science Reviews*, *163*, 193–208. https://doi.org/10.1016/j.quascirev.2017.03.003

Cutler, K. B., Edwards, R. L., Taylor, F. W., Cheng, H., Adkins, J., Gallup, C. D., et al. (2003). Rapid sea-level fall and deep-ocean temperature change since the last interglacial period. *Earth and Planetary Science Letters*, *206*(3–4), 253–271. https://doi.org/10.1016/S0012-821X(02)01107-X

Dalton, A. S., Finkelstein, S. A., Barnett, P. J., & Forman, S. L. (2016). Constraining the Late Pleistocene history of the Laurentide Ice Sheet by dating the Missinaibi Formation, Hudson Bay Lowlands, Canada. *Quaternary Science Reviews*, *146*, 288–299. https://doi.org/10.1016/j.quascirev.2016.06.015

Dalton, A. S., Finkelstein, S. A., Forman, S. L., Barnett, P. J., Pico, T., & Mitrovica, J. X. (2019). Was the Laurentide Ice Sheet significantly reduced during Marine Isotope Stage 3?. *Geology*, *47*(2), 111–114. https://doi.org/10.1130/G45335.1

Deser, C., & Wallace, J. M. (1990). Large-scale atmospheric circulation features of warm and cold episodes in the tropical Pacific. *Journal of Climate*, *3*(11), 1254–1281. https://doi.org/10.1175/1520-0442(1990)003%3C1254:LSACFO%3E2.0.CO;2

Diefendorf, A. F., Mueller, K. E., Wing, S. L., Koch, P. L., & Freeman, K. H. (2010). Global patterns in leaf ^{13}C discrimination and implications for studies of past and future climate. *Proceedings of the National Academy of Sciences of the United States of America*, *107*(13), 5738–5743. https://doi.org/10.1073/pnas.0910513107

DiNezio, P. N., Clement, A., Vecchi, G. A., Soden, B., Broccoli, A. J., Otto-Bliesner, B. L., & Braconnot, P. (2011). The response of the Walker circulation to Last Glacial Maximum forcing: Implications for detection in proxies. *Paleoceanography*, *26*, PA3217. https://doi.org/10.1029/2010PA002083

DiNezio, P. N., & Tierney, J. E. (2013). The effect of sea level on glacial Indo-Pacific climate. *Nature Geoscience*, *6*(6), 485–491. https://doi.org/10.1038/ngeo1823

DiNezio, P. N., Tierney, J. E., Otto-Bliesner, B. L., Timmermann, A., Bhattacharya, T., Rosenbloom, N., & Brady, E. (2018). Glacial changes in tropical climate amplified by the Indian Ocean. *Science Advances*, *4*(12), eaat9658. https://doi.org/10.1126/sciadv.aat9658

DiNezio, P. N., Timmermann, A., Tierney, J. E., Jin, F.-F., Otto-Bliesner, B., Rosenbloom, N., et al. (2016). The climate response of the Indo-Pacific warm pool to glacial sea level. *Paleoceanography*, *31*, 866–894. https://doi.org/10.1002/2015PA002890

Donohoe, A., Marshall, J., Ferreira, D., & Mcgee, D. (2013). The relationship between ITCZ location and cross-equatorial atmospheric heat transport: From the seasonal cycle to the Last Glacial Maximum. *Journal of Climate*, *26*(11), 3597–3618. https://doi.org/10.1175/JCLI-D-12-00467.1

Dubois, N., Oppo, D. W., Galy, V. V., Mohtadi, M., van der Kaars, S., Tierney, J. E., et al. (2014). Indonesian vegetation response to changes in rainfall seasonality over the past 25,000 years. *Nature Geoscience*, *7*(7), 513–517. https://doi.org/10.1038/NGEO2182

Ehlerginger, J. R., Cerling, T. E., & Helliker, B. R. (1997). C_4 photosynthesis, atmospheric CO_2, and climate. *Oecologia*, *112*(3), 285–299. https://doi.org/10.1007/s004420050311

Garcin, Y., Vincens, A., Williamson, D., Guiot, J., & Buchet, G. (2006). Wet phases in tropical southern Africa during the last glacial period. *Geophysical Research Letters*, *33*, L07703. https://doi.org/10.1029/2005GL025531

Griffiths, M. L., Drysdale, R. N., Gagan, M. K., Zhao, J. X., Ayliffe, L. K., Hellstrom, J. C., et al. (2009). Increasing Australian–Indonesian monsoon rainfall linked to early Holocene sea-level rise. *Nature Geoscience*, *2*(9), 636–639. https://doi.org/10.1038/ngeo605

Hendon, H. (2003). Indonesian rainfall variability: Impacts of ENSO and local air–sea interaction. *Journal of Climate*, *16*(11), 1775–1790. https://doi.org/10.1175/1520-0442(2003)016%3C1775:IRVIOE%3E2.0.CO;2

Johnston, P. (1993). The effect of spatially non-uniform water loads on prediction of sea-level change. *Geophysical Journal International*, *114*(3), 615–634. Available at:. http://onlinelibrary.wiley.com/doi/10.1111/j.1365-246X.1993.tb06992.x/abstract

Jones, T. R., Roberts, W. H. G., Steig, E. J., Cuffey, K. M., Markle, B. R., & White, J. W. C. (2018). Southern Hemisphere climate variability forced by Northern Hemisphere ice-sheet topography. *Nature*, *554*(7692), 351–355. https://doi.org/10.1038/nature24669

Kendall, R. A., Mitrovica, J. X., & Milne, G. A. (2005). On post-glacial sea level—II. Numerical formulation and comparative results on spherically symmetric models. *Geophysical Journal International*, *161*(3), 679–706. https://doi.org/10.1111/j.1365-246X.2005.02553.x

Konecky, B., Russell, J., & Bijaksana, S. (2016). Glacial aridity in central Indonesia coeval with intensified monsoon circulation. *Earth and Planetary Science Letters*, *437*, 15–24. https://doi.org/10.1016/j.epsl.2015.12.037

Krause, C. E., Gagan, M. K., Dunbar, G. B., Hantoro, W. S., Hellstrom, J. C., Cheng, H., et al. (2019). Spatio-temporal evolution of Australasian monsoon hydroclimate over the last 40,000 years. *Earth and Planetary Science Letters*, *513*, 103–112. https://doi.org/10.1016/j.epsl.2019.01.045

Lambeck, K., & Chappell, J. (2001). Sea level change through the last glacial cycle. *Science (New York, N.Y.)*, *292*(5517), 679–686. https://doi.org/10.1126/science.1059549

Lambeck, K., Purcell, A., Johnston, P., Nakada, M., & Yokoyama, Y. (2003). Water-load definition in the glacio-hydro-isostatic sea-level equation. *Quaternary Science Reviews*, *22*(2–4), 309–318. https://doi.org/10.1016/S0277-3791(02)00142-7

Lee, S.-Y., Chiang, J. C. H., & Chang, P. (2015). Tropical Pacific response to continental ice sheet topography. *Climate Dynamics*, *44*(9–10), 2429–2446. https://doi.org/10.1007/s00382-014-2162-0

Liu, J., Saito, Y., Wang, H., Zhou, L., & Yang, Z. (2009). Stratigraphic development during the Late Pleistocene and Holocene offshore of the Yellow River delta, Bohai Sea. *Journal of Asian Earth Sciences*, *36*(4–5), 318–331. https://doi.org/10.1016/j.jseaes.2009.06.007

Luthi, D., Le Floch, M., Bereiter, B., Blunier, T., Barnola, J.-M., Siegenthaler, U., et al. (2008). High-resolution carbon dioxide concentration record. *Nature*, *453*(7193), 379–382. https://doi.org/10.1038/nature06949

Macdonald, F. A., Swanson-Hysell, N. L., Park, Y., Lisiecki, L., & Jagoutz, O. (2019). Arc-continent collisions in the tropics set Earth's climate state. *Science*, *184*, 181–184.

Marshall, J. D., Brooks, J. R., & Lajtha, K. (2008). Sources of variation in the stable isotopic composition of plants. In *Stable isotopes in ecology and environmental science: Second edition* (pp. 22–60). Hoboken, NJ: Blackwell Publishing Ltd. https://doi.org/10.1002/9780470691854.ch2

McGee, D. (2020). Glacial–interglacial precipitation changes. *Annual Review of Marine Science*, 1–33.

Meckler, A. N., Clarkson, M. O., Cobb, K. M., Sodemann, H., & Adkins, J. F. (2012). Interglacial hydroclimate in the tropical West Pacific through the Late Pleistocene. *Science*, *6961*(June), 1301–1305.

Milliman, J. D., & Farnsworth, K. L. (2011). *River discharge to the coastal ocean: A global synthesis*. Cambridge, UK: Cambridge Univ. Press. https://doi.org/10.1017/CBO9780511781247

Milne, G. A., & Mitrovica, J. X. (1996). Postglacial sea-level change on a rotating Earth: First results from a gravitationally self-consistent sea-level equation. *Geophysical Journal International*, *126*(3), F13–F20. https://doi.org/10.1111/j.1365-246X.1996.tb04691.x

Milne, G. A., Mitrovica, J. X., & Davis, J. L. (1999). Near-field hydro-isostasy: The implementation of a revised sea-level equation. *Geophysical Journal International*, *139*(2), 464–482. https://doi.org/10.1046/j.1365-246x.1999.00971.x

Mitrovica, J. X., & Milne, G. A. (2002). On the origin of late Holocene sea-level highstands within equatorial ocean basins. *Quaternary Science Reviews*, *21*(20–22), 2179–2190. https://doi.org/10.1016/S0277-3791(02)00080-X

Mitrovica, J. X., Wahr, J., Matsuyama, I., & Paulson, A. (2005). The rotational stability of an ice-age earth. *Geophysical Journal International*, *161*(2), 491–506. https://doi.org/10.1111/j.1365-246X.2005.02609.x

Molnar, P., & Cronin, T. W. (2015). Growth of the Maritime Continent and its possible contribution to recurring Ice Ages. *Paleoceanography*, *30*, 196–225. https://doi.org/10.1002/2014PA002752

Partin, J. W., Cobb, K. M., Adkins, J. F., Clark, B., & Fernandez, D. P. (2007). Millennial-scale trends in west Pacific warm pool hydrology since the Last Glacial Maximum. *Nature*, *449*(7161), 452–455. https://doi.org/10.1038/nature06164

Peltier, W. R., & Fairbanks, R. G. (2006). Global glacial ice volume and Last Glacial Maximum duration from an extended Barbados sea level record. *Quaternary Science Reviews*, *25*(23-24), 3322–3337. https://doi.org/10.1016/j.quascirev.2006.04.010

Pico, T., Creveling, J. R., & Mitrovica, J. X. (2017). Sea-level records from the U.S. mid-Atlantic constrain Laurentide Ice Sheet extent during Marine Isotope Stage 3. *Nature Communications*, *8*, 15612. https://doi.org/10.1038/ncomms15612

Pico, T., Mitrovica, J. X., Ferrier, K. L., & Braun, J. (2016). Global ice volume during MIS 3 inferred from a sea-level analysis of sedimentary core records in the Yellow River Delta. *Quaternary Science Reviews*, *152*, 72–79. https://doi.org/10.1016/j.quascirev.2016.09.012

Reeves, J. M., Barrows, T. T., Cohen, T. J., Kiem, A. S., Bostock, H. C., Fitzsimmons, K. E., et al. (2013). Climate variability over the last 35,000 years recorded in marine and terrestrial archives in the Australian region: An OZ-INTIMATE compilation. *Quaternary Science Reviews*, *74*, 21–34. https://doi.org/10.1016/j.quascirev.2013.01.001

Russell, J. M., Vogel, H., Konecky, B. L., Bijaksana, S., Huang, Y., Melles, M., et al. (2014). Glacial forcing of central Indonesian hydroclimate since 60,000 y B.P. *Proceedings of the National Academy of Sciences*, *111*(14), 5100–5105. https://doi.org/10.1073/pnas.1402373111

Schilt, A., Baumgartner, M., Schwander, J., Buiron, D., Capron, E., Chappellaz, J., et al. (2010). Atmospheric nitrous oxide during the last 140,000 years. *Earth and Planetary Science Letters*, *300*(1-2), 33–43. https://doi.org/10.1016/j.epsl.2010.09.027

Siddall, M., Rohling, E. J., Thompson, W. G., & Waelbroeck, C. (2008). Marine isotope stage 3 sea level fluctuations: Data synthesis and new outlook'. *Reviews of Geophysics*, *46*, RG4003. https://doi.org/10.1029/2007RG000226.1

Tierney, J. E., Peter, B., & Zander, P. D. (2017). A climatic context for the out-of-Africa migration. *Geology*, *45*(11), 1023–1026. https://doi.org/10.1130/G39457.1

Timmermann, A., Lorenz, S. J., An, S. I., Clement, A., & Xie, S. P. (2007). The effect of orbital forcing on the mean climate and variability of the tropical Pacific. *Journal of Climate*, *20*(16), 4147–4159. https://doi.org/10.1175/JCLI4240.1

Vogts, A., Moossen, H., Rommerskirchen, F., & Rullkötter, J. (2009). Distribution patterns and stable carbon isotopic composition of alkanes and alkan-1-ols from plant waxes of African rain forest and savanna C_3 species. *Organic Geochemistry*, *40*(10), 1037–1054. https://doi.org/10.1016/j.orggeochem.2009.07.011

Waelbroeck, C., Labeyrie, L., Michel, E., Duplessy, J. C., McManus, J. F., Lambeck, K., et al. (2002). Sea-level and deep water temperature changes derived from benthic foraminifera isotopic records. *Quaternary Science Reviews*, *21*(1–3), 295–305. https://doi.org/10.1016/S0277-3791(01)00101-9

Walker, J. C. G., Hays, P. B., & Kasting, J. F. (1981). A negative feedback mechanism for the long-term stabilization of Earth's surface temperature. *Journal of Geophysical Research*, *86*(C10), 9776–9782. https://doi.org/10.1029/JC086iC10p09776

Wicaksono, S. A., Russell, J. M., & Bijaksana, S. (2015). Compound-specific carbon isotope records of vegetation and hydrologic change in central Sulawesi, Indonesia, since 53,000 yr BP. *Palaeogeography, Palaeoclimatology, Palaeoecology*, *430*, 47–56. https://doi.org/10.1016/j.palaeo.2015.04.016

Wicaksono, S. A., Russell, J. M., Holbourn, A., & Kuhnt, W. (2017). Hydrological and vegetation shifts in the Wallacean region of central Indonesia since the Last Glacial Maximum. *Quaternary Science Reviews*, *157*, 152–163. https://doi.org/10.1016/j.quascirev.2016.12.006

Windler, G., Tierney, J. E., DiNezio, P. N., Gibson, K., & Thunell, R. (2019). Shelf exposure influence on Indo-Pacific Warm Pool climate for the last 450,000 years. *Earth and Planetary Science Letters*, *516*, 66–76. https://doi.org/10.1016/j.epsl.2019.03.038